

Time-lapse misorientation maps for the analysis of electron backscatter diffraction data from evolving microstructures

J. Wheeler,^{a,*} A. Cross,^a M. Drury,^b R.M. Hough,^c E. Mariani,^a S. Piazzolo^d and D.J. Prior^{a,1}

^aDepartment of Earth and Ocean Sciences, School of Environmental Science, Liverpool University, Liverpool L69 3GP, UK

^bDepartment of Earth Sciences, Utrecht University, P.O.B. 80021, NL-3508 TA Utrecht, Netherlands

^cCSIRO Earth Sciences and Resource Engineering, Kensington, Perth, Australia

^dDepartment of Geosciences, Macquarie University, NSW 2109, Australia

Received 31 March 2011; revised 10 May 2011; accepted 24 June 2011

Available online 29 June 2011

A “time-lapse misorientation map” is defined here as a map which shows the orientation change at each point in an evolving crystalline microstructure between two different times. Electron backscatter diffraction data from in situ heating experiments can be used to produce such maps, which then highlight areas of microstructural change and also yield statistics indicative of how far different types of boundary (with different misorientations) have moved.

© 2011 Acta Materialia Inc. Published by Elsevier Ltd. All rights reserved.

Keywords: Electron backscatter diffraction; Orientation mapping; Misorientation; Grain coarsening; Annealing

The microstructures of crystalline materials control their properties. An understanding of how microstructures develop is important in metallurgy so as to point the way to improved manufacturing pathways, and in rocks so as to deduce their histories of heating and deformation from “post mortem” observations. A direct way of investigating microstructural evolution is to make repeated observations on a sample as it is subject to treatment [1]. Commonly heating is involved, and the sample may either be repeatedly heated and quenched, with ex situ observations following each quench, or heated and observed in situ [2]. Electron backscatter diffraction (EBSD) has proved an invaluable tool in characterizing microstructures; this century EBSD mapping has become routine. The CamScan X500 SEM at Liverpool has a horizontal stage and tilted beam column, a geometry offering certain advantages for EBSD analysis in situ during heating experiments [3]. We have studied phase transformation in Ti [4] and recovery, recrystallization and grain coarsening in NaCl [5,6], Ni [7], Al [8], Mg [9,10], Fe [11] and Au (re-

ported below). Results from such experiments are displayed in standard ways (e.g. Euler angle maps, pole figures), and much may be learnt by a qualitative assessment of how the various displays evolve through time. We have found, though, that it requires care to identify the particular areas within maps which are actively evolving at particular times. Moreover, there is much information in the evolving time series that we do not exploit fully. Here we discuss a more formal, quantitative but objective method for comparing EBSD maps from a time series.

EBSD provides crystallite orientation. The misorientation between two measurements is defined as the minimum rotation required to bring one measurement into parallelism with the other. On a particular EBSD map, misorientations between adjacent pixels may indicate the nature of a low-angle boundary. Misorientations between pairs of pixels selected at random can also be used. Now suppose we have two maps taken from the same region at different times (t_1 and t_2) during an experiment. We define here a time-lapse misorientation (TLM) map as a map that shows the orientation change at a given point from time t_1 – t_2 .

Figure 1, left column, gives an example: an extruded rod of the Mg alloy Magnox AL80 (with 0.9% Al, 0.005% Be) was machined, annealed and deformed at

*Corresponding author. Tel.: +44 1517945172; e-mail: johnwh@liv.ac.uk

¹ Present Address: Department of Geology, University of Otago, 360 Leith Walk, Dunedin 9054, New Zealand.

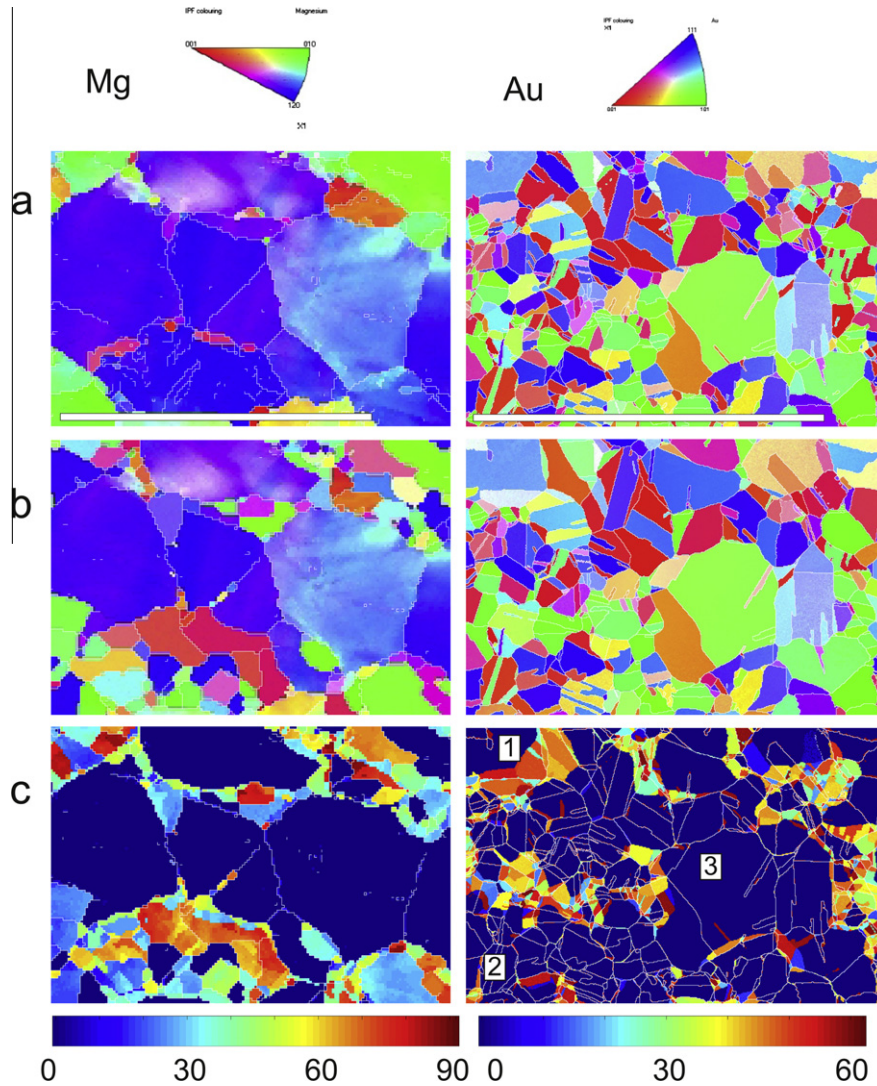


Figure 1. EBSD maps showing microstructural evolution. The left-hand column relates to Mg, the right to Au. (a) Orientation map of the initial microstructure, colour coded according to the relationship of the x direction to the crystallite axes (key above). Scale bar = 500 μm for Mg, 1000 μm for Au. White lines are $>5^\circ$ boundaries. (b) Orientation map after annealing as described in text. (c) The change in orientation between the two upper maps, colour coded as in the colour bar shown below. The boundaries are shown after heating, as in map (b).

$1.9 \times 10^{-4} \text{ s}^{-1}$ to 30% strain at 200 $^\circ\text{C}$ ($0.51 T_m$) [12]. An area was mapped, taken to 200 $^\circ\text{C}$ in three 30 min stages, cooled and mapped again in the Liverpool Cam-Scan X500. The TLM map immediately highlights the regions that have changed. The way in which the map is interpreted depends on the processes involved, but we suppose here that change is being accomplished by the movement of boundaries, whilst material points themselves remain fixed. The orientation of a point changes as a boundary “sweeps” across it, so the TLM map indicates which areas have been swept and provides an indication of the misorientations across moving boundaries.

Figure 2, left column, shows statistics of orientation data from a larger area than that shown in Figure 1, the larger area ($1.56 \times 3 \text{ mm}$) chosen so that statistics will have more significance. The boundary length vs. misorientation is a useful statistic [13]: histograms showing it before and after heating (Figure 2a and b) highlight how low-angle boundaries have been elim-

inated, thus reducing stored energy during recrystallization. Consider now a histogram of area vs. misorientation (θ) derived from the TLM map (Figure 2c), which shows peaks near 30° and 75° . What is the origin of these peaks? They could indicate that boundaries with those misorientations have moved faster than others, or simply that there was a longer total boundary length for those misorientations (as shown in Figure 2a). To quantify these possibilities, imagine first that the elapsed time is small, Δt ; the swept area contributed by a boundary element length Δs is then

$$\Delta A = u(\theta)\Delta s - \Delta t \tag{1}$$

so that

$$\Delta A/\Delta\theta = u(\theta)(\Delta s/\Delta\theta)\Delta t \tag{2}$$

and

$$u(\theta)\Delta t = (\Delta A/\Delta\theta)/(\Delta s/\Delta\theta) \tag{3}$$

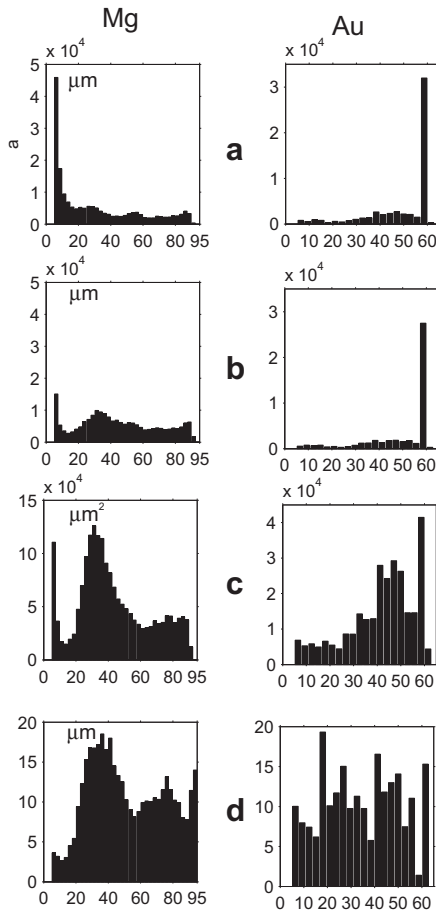


Figure 2. Statistical data related to the microstructural evolution. The left-hand column relates to Mg (a larger region than that shown in Figure 1), the right to Au (the same area as in Figure 1). Boundary length (μm) vs. misorientation for $>5^\circ$ boundaries (a) before heating and (b) after heating. (c) Area swept (μm^2) vs. the orientation change after heating. (d) An indication of the boundary movement (μm) vs. misorientation derived from data in the other histograms; see the text for details.

where $u(\theta)$ is the local movement speed perpendicular to the boundary trace in the plane of the map. This may be a function of misorientation (we focus on this) as well as other factors (e.g. plastic strain energy differences, boundary energy as a function of orientation). The area swept for a small misorientation interval $\Delta\theta$ thus depends on the length of boundary in that misorientation range and the average speed that such boundaries move at. For a finite elapsed time we can estimate the boundary displacement. If the lengths of boundaries have changed during that time interval, consider Figure 3,

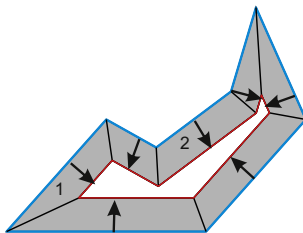


Figure 3. A segmented boundary migrating by a particular displacement amount (shown by arrows) sweeps out the grey area as indicated.

which shows how the swept area relates to boundary geometry for a boundary with the same displacement for each boundary segment. Each segment sweeps out a trapezoidal region. Regardless of whether boundaries are migrating towards their concave (1) or convex (2) sides, each trapezoid has the area:

$$A = \text{Displacement} \times (\text{boundary length before} + \text{boundary length after})/2 \quad (4)$$

By summing the left and right sides of Eq. (4) over all trapezoids, we find that this equation applies also to the total area swept. Hence we obtain an indication of boundary displacement from:

$$\text{Displacement indication} = 2(\text{binned area})/(\text{binned boundary length before} + \text{binned boundary length after}) \quad (5)$$

The result is shown in Figure 2d, a simple proxy for boundary displacement. A peak near 30° remains and one at 75° is quite prominent. We suggest that boundaries with these misorientations migrate faster than others. The peak near 90° relates to very small lengths and areas, so is likely to have a large error and we do not discuss it further.

Figure 1, right column, gives a second example of a TLM map. Natural surface alluvial gold nuggets display internal recrystallization microstructures which can in principle be used to interpret temperatures of formation. To test this idea, an alloy of Au with 30% Ag was deformed to 10% strain by rolling then statically annealed at temperature in the Liverpool CamScan X500. After initial recrystallization, during which many twin boundaries with 60° misorientation developed, the sample was held at 700°C for 16 h. The TLM map shows various features, which are numbered in Figure 1c. Some boundaries have moved towards their concave side, as expected for boundary energy-driven migration (e.g. the bottom right of grain 1). There is an abundance of twin boundaries and these have limited movement (note such boundaries are surrounded by blue, indicating no orientation change and no boundary migration, e.g. grain 2). A slightly concave boundary has moved downwards at the bottom of grain 3. Above it, a slender twin has disappeared, indicating there is some migration of twin boundaries.

Figure 2, right column, shows the corresponding histograms, from the same area as shown in Figure 1. There is an abundance of twin boundaries before and after heating (Fig. 2a and b). The histogram of area swept (Fig. 2c) shows a fairly large area swept by boundaries near 60° , which seems to contradict the inference that twin boundaries are immobile. However, when divided by averaged boundary length (Eq. (5)), the peak becomes a trough (Fig. 2d), underlining the relative immobility of twin boundaries. Other boundaries show no particular pattern in terms of mobility, but studies of a larger area could in principle reveal systematic behaviour (as in the Mg example).

To use this approach, the two (or more) EBSD maps must be registered: we need to ensure that the same material points from the two maps are used for misori-

entation calculation. This is analogous to the problem of registering serial sections for three-dimensional (3-D) data [14]. However, it is less severe because there may be recognizable features which have remained stationary during microstructural evolution, such as scratches and other blemishes, or features introduced deliberately. Locally complicated, recognizable microstructural patterns which persist can also be used, because one cannot envisage an entire collection of ornate boundaries translating en masse without shape change. In practice, we have found that if two maps are misaligned the TLM map is quite diagnostic – for instance, misalignment in the y direction gives rise to a “smearing” effect parallel to y in the TLM map.

For a single boundary, the displacement on a 2-D map will always be equal to or greater than 3-D displacement because of the angle the boundary makes with the map. One can envisage stereological biases if boundaries with particular misorientations also have particular orientations. Such biases will be present in any quantitative analysis of 2-D maps, and we will in future investigate how to deal with them. The deformation histories of the two samples we show here do not imply that there will be any correlation between boundary orientation and misorientation. Although there are stereological and other issues to be addressed as we develop our approach, we have shown that the TLM maps and related histograms are objective displays of microstructural evolution data and provide a stimulus for developing explanatory models.

In summary:

- (1) TLM maps are objective displays of microstructural changes.
- (2) They provide an incremental or cumulative display of orientation through time, enabling easy visualization of where changes are localized.
- (3) They provide quantitative statistics on the areas associated with each orientation change. In some circumstances these will relate to boundary length and/or boundary migration speed vs. misorientation.

We thank the funders of this research, the Natural Environment Research Council (NE/D006600/1 and NE/G01034X/1 to D.J.P./E.M./J.W.) and the European Union for Marie Curie Fellowship HPMF-CT-2001-01457 (Piazolo). CSIRO is thanked for a collaboration fund project with M.D.U. and a Julius award to R.M.H.

- [1] S.I. Wright, M.M. Nowell, in: A.J. Schwartz, M. Kumar, B.L. Adams, D.P. Field (Eds.), *Electron Backscatter Diffraction in Materials Science*, Springer, Berlin, 2009, pp. 329–338.
- [2] P.J. Hurley, F.J. Humphreys, *Journal of Microscopy (Oxford)* 213 (2004) 225–234.
- [3] G.G.E. Seward, D.J. Prior, J. Wheeler, S. Celotto, D.J.M. Halliday, R.S. Paden, M.R. Tye, *Scanning* 24 (2002) 232–240.
- [4] G.G.E. Seward, S. Celotto, D.J. Prior, J. Wheeler, R.C. Pond, *Acta Materialia* 52 (2004) 821–832.
- [5] M. Bestmann, S. Piazolo, C.J. Spiers, D.J. Prior, *Journal of Structural Geology* 27 (2005) 447–457.
- [6] S. Piazolo, M. Bestmann, D.J. Prior, C.J. Spiers, *Tectonophysics* 427 (2006) 55–71.
- [7] S. Piazolo, M.W. Jessell, D.J. Prior, P.D. Bons, *Journal of Microscopy (Oxford)* 213 (2004) 273–284.
- [8] S. Piazolo, V.G. Sursaeva, D.J. Prior, *Zeitschrift Fur Metallkunde* 96 (2005) 1152–1157.
- [9] S. Piazolo, M. Drury, D. Prior, in: *Proceedings of the CHANNEL Users Meeting 2004*, HKL Technology, Ribe, 2004, pp. 50–55.
- [10] J. Wheeler, E. Mariani, S. Piazolo, D.J. Prior, P. Trimby, M.R. Drury, *Journal of Microscopy* 233 (2009) 482–494.
- [11] N.C.A. Seaton, D.J. Prior, in: B. Bacroix, J.H. Driver, R. LeGall, C. Maurice, R. Penelle, H. Regle, L. Tabourot (Eds.), *Recrystallization and Grain Growth*, Pts. 1 and 2, Trans Tech publications Ltd, Switzerland, 2004, pp. 93–98.
- [12] S.E. Ion, F.J. Humphreys, S.H. White, *Acta Metallurgica* 30 (1982) 1909–1919.
- [13] J. Wheeler, Z. Jiang, D.J. Prior, J. Tullis, M. Drury, P.J. Trimby, *Tectonophysics* 376 (2003) 19–35.
- [14] M.A. Groeber, D.J. Rowenhorst, M.D. Uchic, in: A.J. Schwartz, M. Kumar, B.L. Adams, D.P. Field (Eds.), *Electron Backscatter Diffraction in Materials Science*, Springer, Berlin, 2009, pp. 123–138.